THE JOURNAL OF PHYSICAL CHEMISTRY B

Article

pubs.acs.org/JPCB

Vibrational Assignment of the Ultrafast Infrared Spectrum of the Photoactivatable Flavoprotein AppA

Allison Haigney,[†] Andras Lukacs,[‡] Richard Brust,[†] Rui-Kun Zhao,[‡] Michael Towrie,[§] Gregory M. Greetham,[§] Ian Clark,[§] Boris Illarionov,[¶] Adelbert Bacher,[⊥] Ryu-Ryun Kim,[¶] Markus Fischer,[¶] Stephen R. Meech,*[,‡] and Peter J. Tonge*[,†]

[†]Department of Chemistry, Stony Brook University, Stony Brook, New York 11794-3400, United States

[‡]School of Chemical Sciences and Pharmacy, University of East Anglia, Norwich NR4 7TJ, U.K.

[§]Central Laser Facility, Harwell Science and Innovation Campus, Didcot, Oxon OX11 0QX, U.K.

[⊥]Lehrstuhl für Organische Chemie und Biochemie, Technische Universität München, D-85747 Garching, Germany

[¶]Institut für Biochemie und Lebensmittelchemie, Universität Hamburg, Grindelallee 117, D-20146 Hamburg, Germany

Supporting Information

ABSTRACT: The blue light using flavin (BLUF) domain proteins, such as the transcriptional antirepressor AppA, are a novel class of photosensors that bind flavin noncovalently in order to sense and respond to high-intensity blue (450 nm) light. Importantly, the noncovalently bound flavin chromophore is unable to undergo large-scale structural change upon light absorption, and thus there is significant interest in understanding how the BLUF protein matrix senses and responds to flavin photoexcitation. Light absorption is proposed to result in alterations in the hydrogen-bonding network that surrounds the flavin chromophore on an ultrafast time scale, and the structural changes caused by photoexcitation are being probed by vibrational spectroscopy. Here we report ultrafast time-resolved infrared spectra of the AppA BLUF domain ($AppA_{BLUF}$) reconstituted with isotopes of FAD, specifically [U-$^{13}C_{17}$]-FAD, [xylene-$^{13}C_8$]-FAD, [U-$^{15}N_4$]-FAD, and [4-$^{18}O_1$]-FAD both in solution and bound to $AppA_{BLUF}$. This allows for unambiguous assignment of ground- and excited-state modes arising directly from the flavin. Studies of model compounds and DFT calculations of the ground-state vibrational spectra reveal the sensitivity of these modes to their environment, indicating they can be used as probes of structural dynamics.

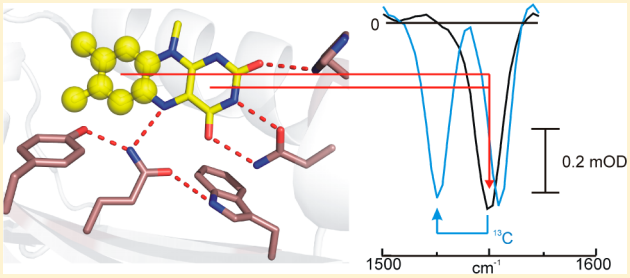

INTRODUCTION

Flavin-containing photoreceptors constitute a unique class of photosensors because they are only able to undergo small structural changes upon light absorption. This is in contrast to the phytochromes, rhodopsins, and xanthopsins where large-scale structural changes, such as a cis−trans isomerization, occur in the chromophore when light is absorbed.[1−3] Thus, flavoprotein photoactivity must arise from other factors, such as electron transfer, hydrogen-bond modulation, or bond formation. Some examples of the known flavin-containing photoreceptors are light-oxygen-voltage (LOV) domain proteins,[4,5] photolyase-like cryptochomes,[6] and the blue-light using FAD (BLUF) domain proteins.[7]

BLUF domain proteins have been found in many species and exhibit a variety of functions. This class of proteins undergoes a characteristic 10 nm red shift in the absorption spectrum of the flavin when excitation with 450 nm light leads to formation of the signaling state. AppA, the best characterized BLUF domain photoreceptor, is found in *Rhodobacter sphaeroides*, where it acts as an antirepressor of photosystem biosynthesis. In the dark, AppA binds PpsR, a transcription factor, forming an AppA−$PpsR_2$ complex. When irradiated with high-intensity blue light, the complex dissociates, releasing PpsR, enabling it to bind to DNA and repress photosystem biosynthesis.[7]

The crystal structure of AppA identifies amino acid residues that form a hydrogen-bonding network around the flavin chromophore. Q63 forms a hydrogen bond to N5 of the flavin ring and also to a conserved tyrosine (Y21) as well as a tryptophan (W104). The glutamine is capable of making two different sets of hydrogen bonds depending on its orientation. It has been postulated that the orientation of Q63 changes upon photoexcitation leading to loss of the hydrogen bond between the glutamine carbonyl and the flavin and disruption of hydrogen bonding with Y21 and W104. Q63 then becomes a hydrogen bond donor to an oxygen atom (O4) on the flavin (Figure 1).[8]

Currently, there is a debate on how the signaling state of AppA is formed. The existing theories differ mainly on the roles of Y21 and Q63 in the photocycle. The first implicates electron transfer from Y21 to the flavin followed by rotation of Q63 as

Received: May 29, 2012
Revised: August 1, 2012
Published: August 7, 2012

dx.doi.org/10.1021/jp305220m | *J. Phys. Chem. B* 2012, 116, 10722−10729

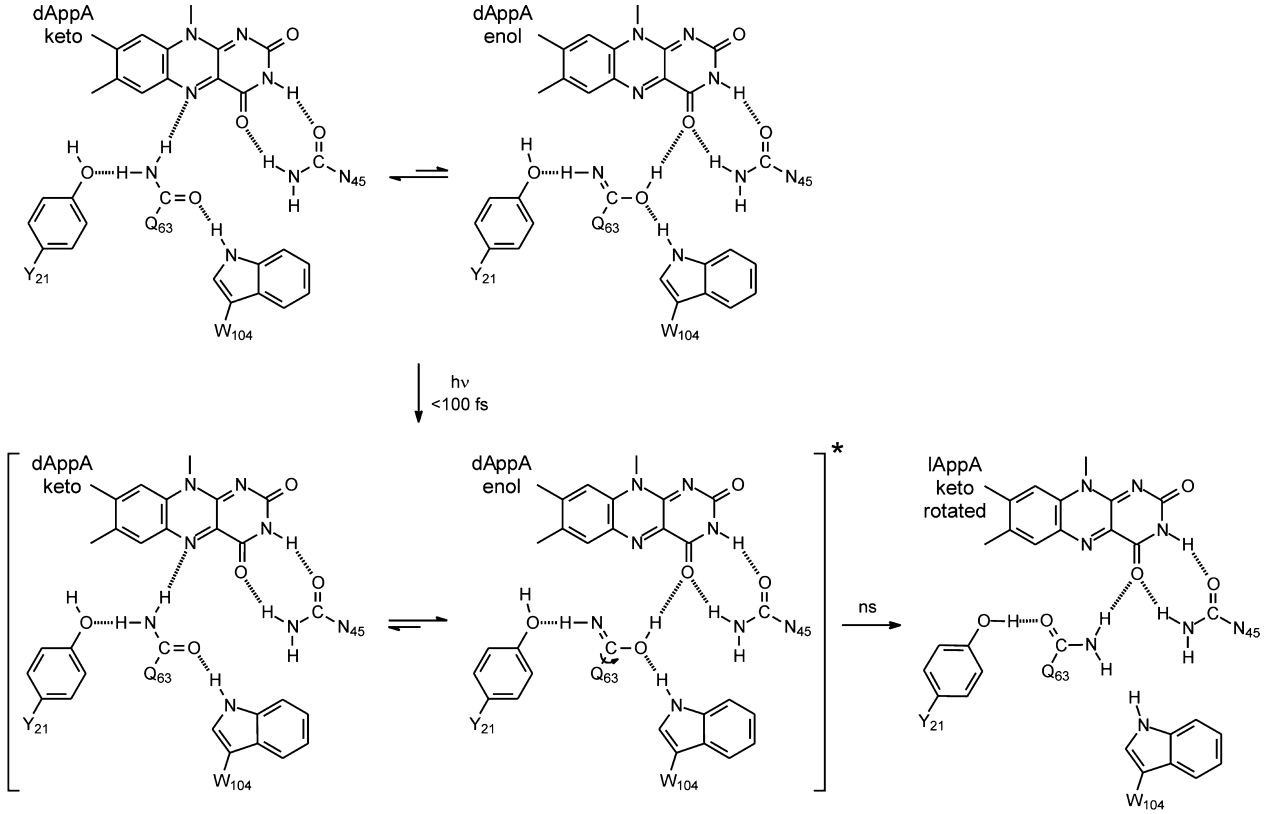

Figure 1. Environment of the isoalloxazine chromophore in AppA. Putative hydrogen-bonding interactions are shown by dashed lines. Photoexcitation involves a tautomerization followed by a rotation of residue Q63 to form lAppA. Reproduced from Lukacs et al.[11]

the first step following blue light excitation,[8] while a second suggests that direct proton transfer from Y21 to N5 of the flavin occurs.[9] In addition, we have proposed instead that keto−enol tautomerism of the Q63 side chain precedes rotation of this residue[10,11] (Figure 1).

The excited-state dynamics of both dark ($dAppA_{BLUF}$) and light ($lAppA_{BLUF}$) adapted states of the AppA BLUF domain have been studied using time-resolved infrared spectroscopy (TRIR). TRIR spectra of unbound flavin were obtained and used to identify ground-state and excited-state vibrational modes. These were compared with TRIR spectra of $dAppA_{BLUF}$ and $lAppA_{BLUF}$. Thus, flavin modes could be separated from modes associated with the protein matrix.[10] These studies showed significant differences between $dAppA_{BLUF}$, $lAppA_{BLUF}$, and free flavin. Most notable was the appearance of a 1666 cm^{-1} transient in $dAppA_{BLUF}$ that is not seen in flavin or $lAppA_{BLUF}$ or in any of the mutants that are photoinactive, suggesting that this is a protein or protein−chromophore mode which is a marker for photoactivity.[10] Here we report TRIR spectra of FAD isotopologues, specifically [U-$^{13}C_{17}$]-FAD, [xylene-$^{13}C_8$]-FAD, [U-$^{15}N_4$]-FAD, and [4-$^{18}O_1$]-FAD both in solution and bound to $AppA_{BLUF}$ (Figure 2), which facilitates a detailed assignment of the vibrational modes in the isoalloxazine ring of the flavin, and further aids the distinction of protein and flavin modes in the congested 1500−1700 cm^{-1} spectral region. In addition, we have used DFT calculations to support our experimental data.

MATERIALS AND METHODS

Materials. FAD (disodium salt) was from Sigma Aldrich. D_2O (99.9 atom %) was from Cambridge Isotope Laboratories.

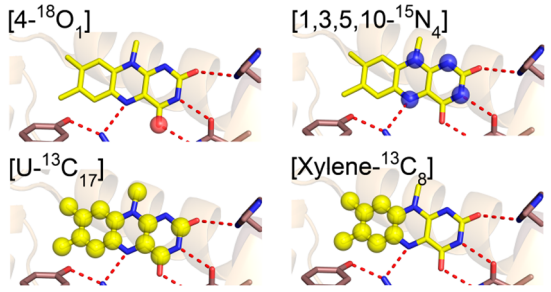

Figure 2. Isotopologues incorporated into AppA: [4-$^{18}O_1$]-FAD, [U-$^{15}N_4$]-FAD, [xylene-$^{13}C_8$]-FAD, and [U-$^{13}C_{17}$]-FAD bound to $AppA_{BLUF}$. The figure was made using pymol.REF.

Ampicillin (disodium salt) was from Fisher Scientific. Ni-NTA resin was from Novagen. ITPG was from GoldChemBio.

Synthesis of FAD Isotopologues. [U-$^{13}C_{17}$]riboflavin, [xylene-$^{13}C_8$]riboflavin, [U-$^{15}N_4$]riboflavin, and [4-$^{18}O_1$]-riboflavin were prepared according to Tishler et al.[12] Riboflavin isotopologues were converted enzymatically to the cognate FAD isotopologues. The purity of each was determined by ESI mass spectrometry (see Supporting Information). Whereas the [U-$^{13}C_{17}$]-FAD, [xylene-$^{13}C_8$]-FAD, and [U-$^{15}N_4$]-FAD were all pure, the [4-$^{18}O_1$]-FAD was determined to be 60% labeled with a 40% contamination of unlabeled FAD. These data are in good agreement with the TRIR measurements where, by comparing the ratio of the 1700 and 1682 cm^{-1} peak intensities, we calculate roughly 60% of the FAD sample is [4-$^{18}O_1$]-FAD (see below).

Protein Expression and Purification. The BLUF domain of AppA ($AppA_{BLUF}$; residues 5−125) was cloned into a pet15b

dx.doi.org/10.1021/jp305220m | J. Phys. Chem. B 2012, 116, 10722−10729

vector (Novagen) so that the protein is expressed with an N-terminal His-tag. Expression and purification were performed using the protocol described previously.[13] The protein was then concentrated to approximately 1 mM, frozen in liquid N_2, and lyophilized overnight. It was then dissolved in the same volume of D_2O to recapitulate the buffer conditions, and incubated at 4 °C for at least 5 h. Full exchange of the protein was accomplished by repeating the lyophilization and addition of D_2O 3 to 4 times, after which the protein samples were stored dry at −20 °C.

Cofactor Exchange. FAD isotopologues were incorporated into $AppA_{BLUF}$ as described previously.[13] Briefly, a 0.68 mM solution (840 μL) of the purified protein in buffer was incubated with 160 μL of 2 mM isotopically labeled FAD in D_2O buffer for 45 min. The solution was concentrated to 400 μL by ultrafiltration. The total volume was adjusted with D_2O buffer to 4 mL and the solution was again concentrated to 400 μL. The dilution/concentration cycle was repeated two more times or until free flavin could not be detected in the eluate. The protein sample (~0.5 mM) was then incubated a second time with an excess of the isotopologue (2 mM), followed by repeated washing until no free flavin could be detected in the protein solution. Using this method, the final percent isotope incorporation was estimated to be greater than 90% which, except for the [4-$^{18}O_1$]-FAD isotopologue, is supported by the absence of vibrational modes in the TRIR spectra associated with the unlabeled FAD.

Time-Resolved Infrared Spectroscopy. Ultrafast transient IR measurements were performed using an ultrastable 10 kHz amplified titanium sapphire laser pumping OPAs for UV to IR pulse generation; the apparatus is described in detail elsewhere.[14] The samples were excited with ~200 nJ linearly polarized pump pulses at 400 nm and probed by broadband IR pulses between 1500 and 1800 cm^{-1}. In order to avoid degradation of the protein and photoconversion of $dAppA_{BLUF}$, a raster sample mover was used in conjunction with a flow cell. In addition, to avoid contributions to the measured dynamics from orientational relaxation, the relative angle between the pump and the probe beams was set to the magic angle (54.7°) using a half-wave plate. The data are presented as IR difference spectra (pumped − unpumped), where negative changes (bleaches) in optical density that appear within the subpicosecond time resolution are assigned to vibrations of the ground state and promptly appearing positive signals (transients) to excited-state modes.

Density Functional Theory Calculations. DFT calculations were carried out on the core chromophore of the isoalloxazine ring, specifically for the molecule lumiflavin, in which the ribityl chain is replaced by a methyl group. In addition, the H atom on N_3 was replaced with a deuterium, since all experiments are performed in D_2O. No specific solvent molecules were included nor was a continuum solvent assumed, so the calculations are strictly relevant to molecules in the gas phase. Our objective in using DFT is to support assignments of the isotopic shifts observed relative to the unlabeled lumiflavin, rather than to provide exact frequencies or information on all of the atomic displacements contributing to the normal modes. All calculations were made using the Gaussian 03 package using a B3LYP functional and the 6-31G+ basis set.[15] Particularly for the carbonyl localized modes, we have found that this basis set underestimates the vibrational frequency compared to experiment. This is even more apparent when the recommended scale factor of 0.96 is applied to the calculated frequencies[16] (as it has been here). This deviation between calculated and experimental data can be corrected by using basis sets which include polarization, and in an earlier study we reported calculations using 6-31G++(d,p).[13] However, we found that this basis set fails to predict even qualitatively the shifts observed in carbonyl localized modes when the N_3H atom is replaced by deuterium. Since all experiments are made in D_2O, this is a serious shortcoming, so the simpler basis set is preferred to calculate the relative shifts in frequency required here.

RESULTS AND DISCUSSION

In addition to our studies on BLUF domain proteins that have primarily utilized TRIR spectroscopy,[10,11,13,17] vibrational spectra of FAD and other flavin analogues, both free in solution and bound to proteins, have previously been obtained using infrared,[18−20] Raman,[21,22] resonance Raman (RR),[20,23−25] and UV RR spectroscopy.[26,27] Assignments for the bands observed in these spectra have previously been proposed based on normal-mode analysis, supplemented in some cases from spectroscopic data on isoalloxazine isotopologues. Labeled compounds previously prepared include the [3-ND], [2-$^{13}C_1$], [4a-$^{13}C_1$], [1,3-$^{15}N_2$], and [1,3,5-$^{15}N_3$] isotopologues of lumiflavin,[18,20] [4-$^{18}O_1$]-lumiflavin, riboflavin, and FAD,[23] and [2-$^{13}C_1$]-FAD and [4,10$_a$-$^{13}C_2$]-riboflavin.[13] On the basis of DFT calculations and polarization-resolved data, we assigned five bands in the TRIR spectrum of FAD in solution at 1703, 1646, 1624, 1578, and 1546 cm^{-1}.[17] In the present paper, we extend these studies to include [4-$^{18}O_1$]-FAD, [U-$^{15}N_4$]-FAD, [xylene-$^{13}C_8$]-FAD, and [U-$^{13}C_{17}$]-FAD, studied in solution and also bound to both d- and l$AppA_{BLUF}$.

FAD Isotopologues in Buffer. The TRIR spectra of FAD and [4-$^{18}O_1$]-FAD measured at a 3 ps time delay after excitation are shown in Figure 3, a and b. The high-frequency bleach at 1700 cm^{-1} in FAD is partially shifted to 1682 cm^{-1} in [4-$^{18}O_1$]-FAD with residual intensity at 1700 cm^{-1}. The ratio of the integrals of the 1700 and 1682 cm^{-1} peaks is in line with the 60% isotope abundance of [4-$^{18}O_1$]-FAD (see Supporting Information), and the higher wavenumber mode is therefore assigned to the C_4═^{16}O stretch. This conclusion is in agreement with previous studies both by us[13,17] and by other workers[18,20,22,26,28] including Nishina et al. who previously assigned a band at 1700 cm^{-1} in the RR spectrum of FAD to the C_4═O flavin mode using [4-$^{18}O_1$]-FAD.[23] The effect of ^{18}O substitution on the mode with the next highest frequency is small, and there is a negligible effect on all the lower frequency modes observed in this spectral window. The DFT calculation shown in Figure 3c is consistent with the observed down shift in the highest frequency mode, but also predicts a similar shift in the second mode (which was shown to be associated with the C_2═O stretch in our earlier study of [2-$^{13}C_1$]riboflavin). The disagreement between calculated and observed carbonyl frequencies was discussed in our earlier paper, and arises from the symmetric and antisymmetric character of the stretching modes associated with the O═C_4—N_3H—C_2═O unit.[13] Typically, gas-phase calculations suggest an assignment of the two highest frequency modes to a symmetric−antisymmetric pair, but, as discussed elsewhere, this is sensitive to the N_3H/D exchange and hydrogen bonding with the environment. The ^{18}O data reported here are consistent with a more localized character for the two C═O stretches in the ground state of

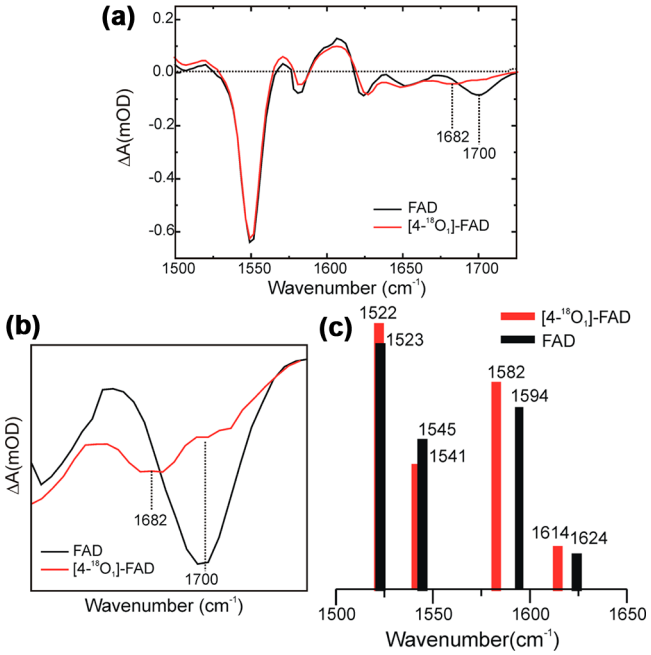

Figure 3. TRIR spectra of unlabeled FAD and [4-$^{18}O_1$]-FAD in D_2O: (a) TRIR spectra of 3 mM FAD (black) and [4-$^{18}O_1$]-FAD (red) in pD 8 phosphate buffer recorded at a time delay of 3 ps. (b) Detail of the carbonyl region of TRIR spectra shown in (a). (c) Calculated spectra of unlabeled FAD (black) and [4-$^{18}O_1$]-FAD (red).

FAD, as was suggested in our study of [4,10*a*-$^{13}C_2$]riboflavin and [2-$^{13}C_1$]riboflavin.[13]

The TRIR spectra of [U-$^{15}N_4$]-FAD and unlabeled FAD are shown in Figure 4. The most significant change that occurs is

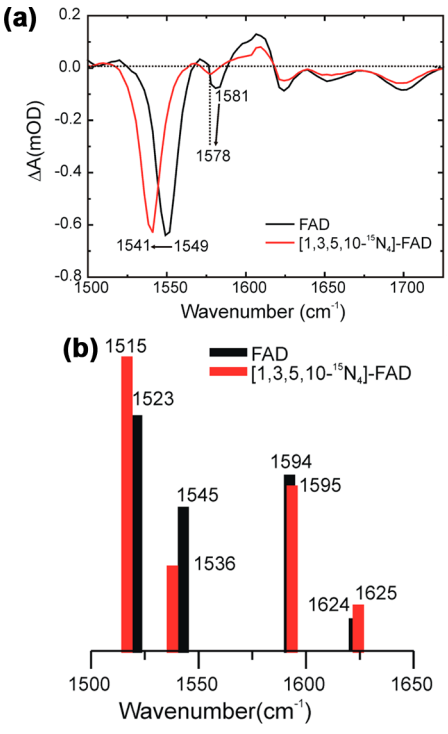

Figure 4. (a) TRIR spectra of unlabeled FAD and [U-$^{15}N_4$]-FAD in D_2O: 3 mM FAD (black) and [U-$^{15}N_4$]-FAD (red) in pD 8 phosphate buffer recorded with a time delay of 3 ps. (b) Calculated spectra of unlabeled FAD (black) and [U-$^{15}N_4$]-FAD (red).

the shift of the 1549 cm^{-1} bleach to 1541 cm^{-1}. The carbonyl modes are hardly altered by exchange of the N atoms. This is in good agreement with DFT calculations (Figure 4b) which show a 8 cm^{-1} shift of the most intense bleach upon uniform ^{15}N labeling. The calculation is summarized in Table 1 where it can be seen that the major contributor to this intense mode is the $C_{10a}N_1$ stretching vibration. In addition, the weaker bleach measured at 1581 cm^{-1} shifts to 1578 cm^{-1} upon ^{15}N labeling, which is also in agreement with the calculated spectra, which in turn suggest that the $C_{4a}N_5$ stretch is a major contributor to this mode. These data are consistent with studies by Kitagawa et al. who observed that bands at 1584 and 1548 cm^{-1} in unlabeled FAD shift to 1580 and 1545 cm^{-1} upon ^{15}N labeling N5 of riboflavin.[20]

Figure 5 shows the TRIR spectra of [xylene-$^{13}C_8$]-FAD. This novel isotopologue has not been previously studied and enables assignment of modes associated with the xylene ring. As can be seen in Figure 5a, upon labeling of the xylene ring an additional bleach appears in the transient IR spectrum, with three intense peaks appearing between 1500 and 1600 cm^{-1}. The carbonyl modes are unaffected by isotopic substitution on the xylene ring. The origin of the extra band can be traced in the DFT calculations (Figure 5b), where the modes at 1545 and 1523 cm^{-1} in FAD are down shifted by 19 cm^{-1} and 29 cm^{-1} respectively. The suggested origin of the band calculated at 1564 cm^{-1} in [xylene-$^{13}C_8$]-FAD is a ring mode with a very weakly allowed IR transition at 1609 cm^{-1} in FAD. Evidently this mode gains considerably in intensity on down shifting, possibly from coupling to more intense modes which include the CN stretch.

The TRIR spectra of [U-$^{13}C_{17}$]-FAD are shown in Figure 6. The 1700 cm^{-1} bleach assigned to the C_4═O is shifted by 40 cm^{-1} to 1660 cm^{-1} which is in agreement with data on the [4,10*a*-$^{13}C_2$] isotopologue studied earlier.[13,29] This shift is also in good agreement with DFT calculations presented in Figure 6b which predict a 44 cm^{-1} shift of this bleach upon uniform ^{13}C labeling of FAD. DFT predicts this to be the symmetric stretch of both carbonyls coupled to the N_3D. As discussed before, the extent to which the mode is in fact one of a symmetric/antisymmetric pair or more localized on a particular C═O stretch depends on the environment. The lower frequency of the bleaches associated with C═O modes, at 1651 cm^{-1}, shifts by approximately 27 cm^{-1} to lower frequency and is observed as a weak bleach mixed with the 1624 cm^{-1} feature (Figure 6a). This is consistent with DFT calculations (Figure 6b) which show a 43 cm^{-1} shift of this bleach upon uniform ^{13}C labeling (Table 1). Other changes observed in the TRIR spectra of [U-$^{13}C_{17}$]-FAD include the 1606 cm^{-1} transient which shifts to approximately 1568 cm^{-1}. This band is assigned to a carbonyl mode in the excited electronic state. Figure 6 also demonstrates that the 1581 and 1549 cm^{-1} bleaches shift to 1536 and 1507 cm^{-1}, respectively, upon uniform ^{13}C labeling of FAD. This is in agreement with these modes having important contributions from CC and CN stretching vibrations. DFT calculations suggest 44 and 34 cm^{-1} shifts in the most intense IR transitions, which are indeed calculated to have significant CN stretching components.

FAD Isotopes Bound to AppA$_{BLUF}$. In Figure 7 TRIR spectra at a 3 ps time delay are shown for dAppA$_{BLUF}$ bound to FAD and [4-$^{18}O_1$]-FAD. The high frequency bleach at 1700 cm^{-1} is partially shifted to 1680 cm^{-1}. This change in peak position is consistent with the 18 cm^{-1} shift seen in the TRIR spectra of [4-$^{18}O_1$]-FAD in buffer. However, the carbonyl

dx.doi.org/10.1021/jp305220m | J. Phys. Chem. B 2012, 116, 10722−10729

Table 1. Observed and Calculated Vibrational Modes of FAD, [4-$^{18}O_1$]-FAD, [U-$^{15}N_4$]-FAD, [U-$^{13}C_{17}$]-FAD, and [xylene-$^{13}C_8$]-FAD in D_2O Buffer[a]

FAD (D_2O)		[4-$^{18}O_1$]-FAD		[U-$^{15}N_4$]-FAD		[uniform-$^{13}C_{17}$]-FAD		[xylene-$^{13}C_8$]-FAD	
obsd (cm^{-1})	calcd (cm^{-1})	obsd (cm^{-1})	calcd (cm^{-1})	obsd (cm^{-1})	calcd (cm^{-1})	obsd (cm^{-1})	calcd (cm^{-1})	obsd (cm^{-1})	calcd (cm^{-1})
1549	1523	1549	1522	1541	1515	1509	1489	1525	1494
	$C_{10a}N_1$		$C_{10a}N_1$		$C_{10a}N_1$		$C_{10a}N_1$		$C_{10a}N_1$, $C_{4a}N_5$ asym
								1554	1526
									$C_{10a}N_1$
1581	1545	1583	1541	1578	1536	1535	1501	1586	1564
	$C_{4a}N_5$		$C_{4a}N_5$		$C_{4a}N_5$		$C_{4a}N_5$		$C_{4a}N_5$
1651	1594	1648	1582	1651	1591	1609	1551	1652	1595
	C_2=O, C_4=O asym +N_3 wag		C_2=O, C_4=O asym +N_3 wag		C_2=O, C_4=O asym +N_3 wag		C_2=O, C_4=O asym +N_3 wag		C_2=O, C_4=O asym +N_3 wag
1699	1624	1685	1614	1700	1622	1660	1580	1700	1625
	C_4=O, C_2=O sym +N_3 wag		C_4=O, C_2=O sym +N_3 wag		C_4=O, C_2=O sym +N_3 wag		C_4=O, C_2=O sym +N_3 wag		C_4=O, C_2=O sym +N_3 wag

[a]Observed frequencies are experimental TRIR measurements. Calculated frequencies were determined by Gaussian 03 using the B3LYP method and 6-31G basis set.

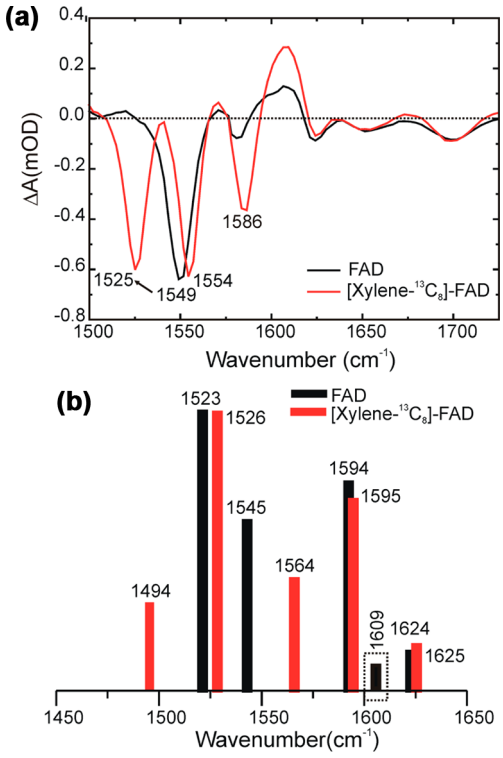

Figure 5. (a) TRIR spectra of unlabeled FAD and [xylene-$^{13}C_8$]-FAD in D_2O: 3 mM FAD (black) and [xylene-$^{13}C_8$]-FAD (red) in pD 8 phosphate buffer recorded with a time delay of 3 ps. (b) Calculated spectra of unlabeled FAD and [xylene-$^{13}C_8$]-FAD: FAD (black) and [xylene-$^{13}C_8$]-FAD (red). The mode at 1609 cm^{-1} has been enhanced by 25×.

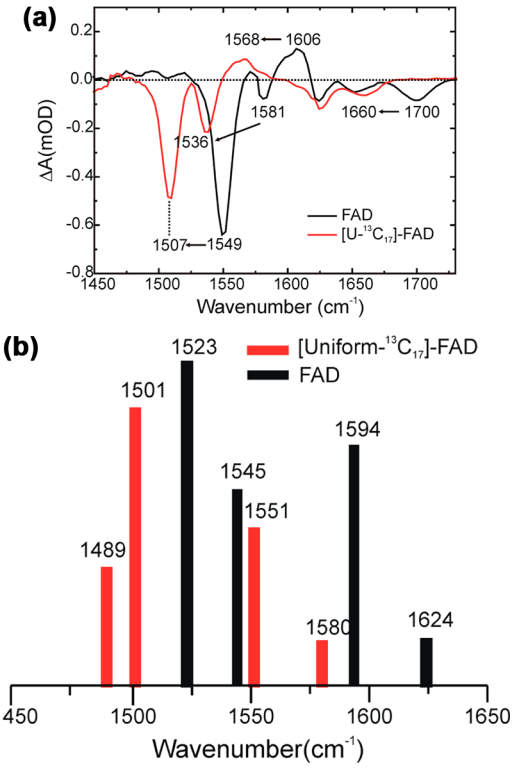

Figure 6. (a) TRIR spectra of unlabeled FAD and [uniform-$^{13}C_{17}$]-FAD in D_2O: 3 mM FAD (black) and [uniform-$^{13}C_{17}$]-FAD (red) in pD 8 phosphate buffer recorded with a time delay of 3 ps. (b) Calculated spectra of unlabeled FAD and [U-$^{13}C_{17}$]-FAD: FAD (black) and [U-$^{13}O_{17}$]-FAD (red).

modes of the flavin are better resolved when bound to $AppA_{BLUF}$. This spectral narrowing was described in our previous paper and is due to restricted hydrogen bonding interactions in the protein compared to FAD in D_2O.[10] In addition, a transient that appears at 1672 cm^{-1} shifts to 1664 cm^{-1} in the spectra of [4-$^{18}O_1$]-FAD bound to $dAppA_{BLUF}$.

The TRIR spectra of unlabeled FAD and [U-$^{15}N_4$]-FAD bound to $AppA_{BLUF}$ are shown in Figure 8. There is a shift of the major bleach at 1549 cm^{-1} to 1539 cm^{-1} in both $dAppA_{BLUF}$ and $lAppA_{BLUF}$ when bound to [U-$^{15}N_4$]-FAD. In addition, the bleach at 1582 cm^{-1} shifts to 1574 cm^{-1}. The changes in the position of the 1549 and 1582 cm^{-1} bands are consistent with the TRIR spectra of solution-phase data, although the shift is greater when [U-$^{15}N_4$]-FAD is bound to $AppA_{BLUF}$ compared to unbound FAD (Figure 4). The major bleach shifts by 10 cm^{-1} when bound to the protein and 8 cm^{-1} in solution and the less intense bleach at 1582 cm^{-1} shifts by 8 cm^{-1} as opposed to the 3 cm^{-1} in solution. Previously, we noted that the character of the flavin vibrational mode is extremely dependent on the hydrogen-bonding environment.

dx.doi.org/10.1021/jp305220m | J. Phys. Chem. B 2012, 116, 10722−10729

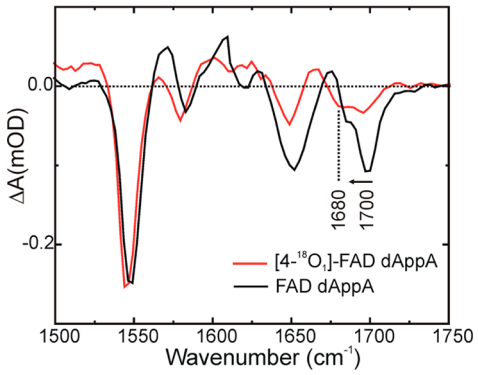

Figure 7. TRIR spectra of unlabeled FAD and [4-$^{18}O_1$]-FAD bound to $AppA_{BLUF}$: 3 mM FAD (black) and [4-$^{18}O_1$]-FAD (red) bound to $dAppA_{BLUF}$ in pD 8 phosphate buffer recorded with a time delay of 3 ps.

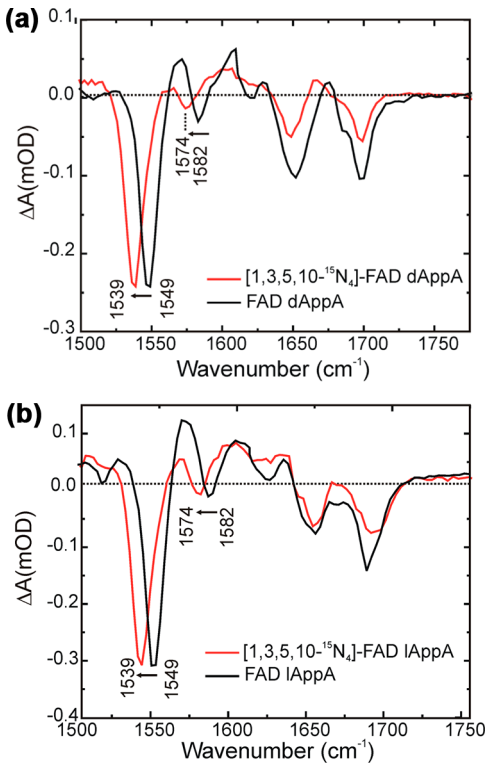

Figure 8. TRIR spectra of unlabeled FAD and [U-$^{15}N_4$]-FAD bound to $AppA_{BLUF}$: 3 mM FAD (black) and [U-$^{15}N_4$]-FAD (red) bound to $dAppA_{BLUF}$ (a) and $lAppA_{BLUF}$ (b) in pD 8 phosphate buffer recorded with a time delay of 3 ps.

This is particularly true for the carbonyl modes. Therefore, we speculate that the different isotope shifts observed for FAD between buffer solution and bound in the protein reflect an environment sensitivity of the character of the CN/CC ring modes as well.

Figure 9 shows the TRIR spectra of unlabeled FAD and [xylene-$^{13}C_8$]-FAD bound to $AppA_{BLUF}$. The spectra are consistent with those seen in buffer, with an enhanced signal at 1570 cm^{-1} assigned to a ring mode with increased intensity. Again, the spectra are somewhat better resolved than in buffer solution because of restricted hydrogen-bonding interactions in the protein. The isotope shifts are consistent between $dAppA_{BLUF}$ and $lAppA_{BLUF}$, where three intense peaks appear between 1500 and 1600 cm^{-1}. In addition to the large bleach

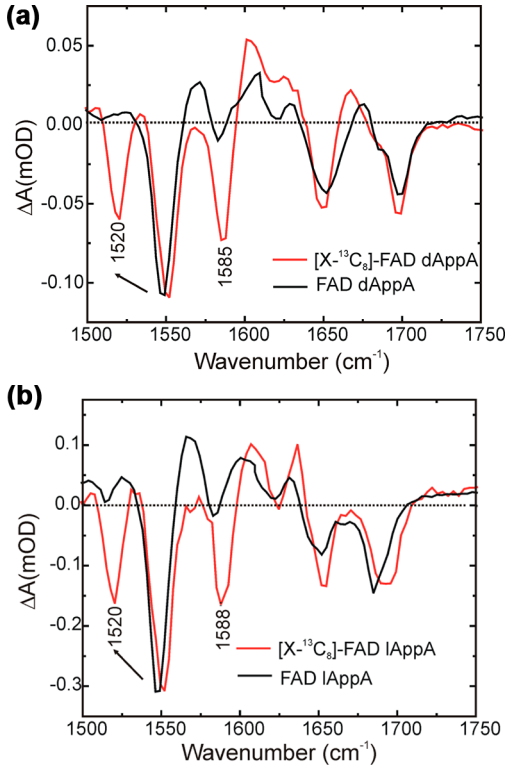

Figure 9. TRIR spectra of unlabeled FAD and [xylene-$^{13}C_8$]-FAD bound to $AppA_{BLUF}$: 3 mM FAD (black) and [xylene-$^{13}C_8$]-FAD (red) bound to $dAppA_{BLUF}$ (a) and $lAppA_{BLUF}$ (b) in pD 8 phosphate buffer recorded with a time delay of 3 ps.

which is now at 1552 cm^{-1}, a new mode is seen at 1520 cm^{-1}. This is essentially as observed in solution (Figure 5) with the additional mode arising from an intensity enhancement resulting from the isotope shift. Finally, as observed in the unbound isotope spectra of [xylene-$^{13}C_8$]-FAD, the carbonyl modes are not affected by isotopic substitution on the xylene ring.

The TRIR spectra of [U-$^{13}C_{17}$]-FAD and unlabeled FAD bound to $AppA_{BLUF}$ at a 3 ps time delay are shown in Figure 10. For both $dAppA_{BLUF}$ and $lAppA_{BLUF}$, the intense bleach at 1549 cm^{-1} shifts by 44 cm^{-1} to 1505 cm^{-1} and the 1582 cm^{-1} bleach shifts to 1536 cm^{-1}. These are consistent with the change in frequency seen upon labeling of FAD in solution (Figure 6). Other shifts are observed in the TRIR spectra of [U-$^{13}C_{17}$]-FAD bound to $AppA_{BLUF}$ but are different for $dAppA_{BLUF}$ and $lAppA_{BLUF}$, and therefore the changes seen in isotope substitution will be discussed separately.

Figure 10a shows [U-$^{13}C_{17}$]-FAD and unlabeled FAD bound to $dAppA_{BLUF}$. The high frequency bleach at 1700 cm^{-1} shifts by 30 cm^{-1} to 1670 cm^{-1}. This change in frequency is similar to that observed previously when $dAppA_{BLUF}$ is reconstituted with [4,10*a*-$^{13}C_2$]-riboflavin,[13] corroborating the assignment of the 1700 cm^{-1} band to the FAD C_4=O carbonyl. The alteration in frequency is smaller when [U-$^{13}C_{17}$]-FAD is bound to $dAppA_{BLUF}$ (30 cm^{-1}) compared to the value observed for the isotopologue in buffer solution (40 cm^{-1}) (Figure 6), which is attributed to the sensitivity of the carbonyl vibrational mode to the hydrogen-bonding environment, as discussed elsewhere.[30] In addition, the 1650 cm^{-1} mode shifts to lower frequency but because of the poor signal-to-noise in this region we are unable to determine the peak position upon labeling.

dx.doi.org/10.1021/jp305220m | J. Phys. Chem. B 2012, 116, 10722−10729

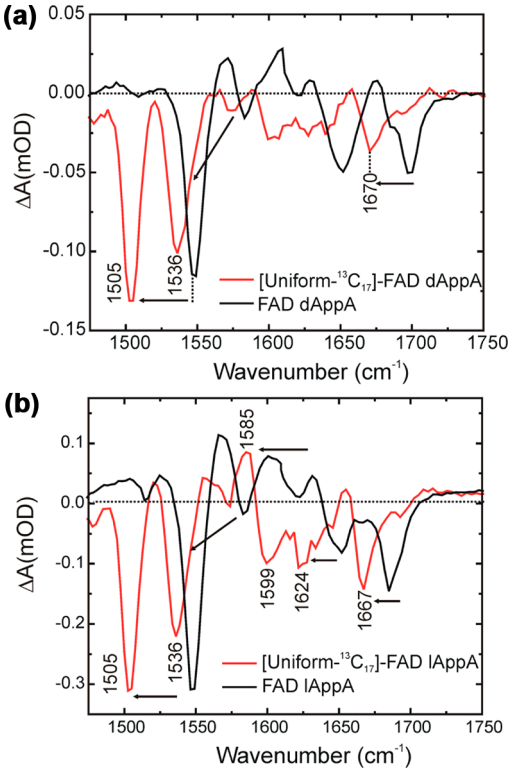

Figure 10. TRIR spectra of unlabeled FAD and [uniform-$^{13}C_{17}$]-FAD bound to $AppA_{BLUF}$: 3 mM FAD (black) and [uniform-$^{13}C_{17}$]-FAD (red) bound to $dAppA_{BLUF}$ (a) and $lAppA_{BLUF}$ (b) in pD 8 phosphate buffer recorded with a time delay of 3 ps.

Figure 10b shows the spectra for [U-$^{13}C_{17}$]-FAD bound to $lAppA_{BLUF}$ in comparison to unlabeled FAD. In these spectra, it is seen that the high (1682 cm^{-1}) and low (1650 cm^{-1}) frequency modes shift by 15 cm^{-1} to 1667 cm^{-1} and 26 cm^{-1} to 1624 cm^{-1} upon ^{13}C labeling, respectively. The sensitivity of these modes to ^{13}C labeling is again in agreement with their assignment to the FAD C_4=O and C_2=O groups, respectively, and with data reported previously for $lAppA_{BLUF}$ bound to [4,10*a*-$^{13}C_2$]-riboflavin and [2-$^{13}C_1$]-FAD.[13] The sensitivity of the $lAppA_{BLUF}$ C_4=O carbonyl mode to labeling is smaller than the shift seen when [U-$^{13}C_{17}$]-FAD is unbound or when it is bound to $dAppA_{BLUF}$ (30 cm^{-1}). This again reflects the high sensitivity of the carbonyl vibrational mode to the hydrogen-bonding environment which is very different for the C_4=O modes of d- and $lAppA_{BLUF}$ due to a strengthening of hydrogen bonding upon formation of the $lAppA_{BLUF}$ from $dAppA_{BLUF}$.[31] Other shifts observed in the TRIR spectra of [U-$^{13}C_{17}$]-FAD bound to $dAppA_{BLUF}$ include the excited-state transient at 1631/1603 cm^{-1} that shifts by approximately 45 cm^{-1} to 1585/1554 cm^{-1}.

TRIR in Comparison to Other Methods. In the current article, we extend our studies on the vibrational spectroscopy of $AppA_{BLUF}$ using the [4-$^{18}O_1$]-FAD, [U-$^{15}N_4$]-FAD, and [xylene-$^{13}C_8$]-FAD isotopologues. While specific isotope shifts are described above, the TRIR data further demonstrate the sensitivity of flavin vibrational modes to environment including those associated with the C_2=O and C_4=O groups. This analysis also reinforces the utility of TRIR spectroscopy, not only for providing explicit data on excited state reactions but also more generally on the usefulness of this technique for obtaining the vibrational spectrum of chromophoric ligands bound to proteins. Vibrational spectra of flavins and flavoproteins, as well as other protein−ligand systems, have traditionally been obtained using steady-state IR, Raman, and RR spectroscopies. For protein−chromophore systems, (pre-resonance) Raman and RR spectroscopies are the usual methods of choice since they provide some selective advantage for detecting modes associated with the isoalloxazine chromophore. RR is very powerful in this regard, but is hampered by the strong fluorescence background normally associated with the flavin chromophore. In addition, neither Raman nor RR spectroscopy are ideal methods for visualizing carbonyl modes, which tend to give weak bands in Raman spectra. In contrast, whereas IR is an ideal method for studying carbonyl modes, this approach is hampered by the strong amide I band that often obscures the region of interest so that carbonyl vibrational modes can only be observed by isotope editing.[32] TRIR combines the selectivity associated with RR spectroscopy with the sensitivity and signal averaging ability of steady-state IR spectroscopy, allowing vibrational modes associated with the electronic transition to be observed in light minus dark difference spectra. Bleaches in the TRIR spectra are ground-state modes from the chromophore or protein residues perturbed by electronic excitation, while transient absorptions are the corresponding excited modes or new ground-state modes perturbed by photoexcitation. Often the excited-state modes are strongly shifted and rather broad, presumably as a result of changes in electronic structure and vibrational coupling. Unfortunately, the calculation of excited-state vibrational spectra for large molecules is not sufficiently accurate to be used as an aid to assignment. As a result of these factors, there are a preponderance of bleaches compared to transients in the TRIR spectra. The current TRIR picosecond system provides information on structural changes that occur instantaneously upon photoexcitation or on the subnanosecond time scale. However, slower structural changes on the biologically relevant microsecond to millisecond time scale will become accessible as we extend our observations to longer time domains. Central to current and future studies will be the ability to introduce selective isotopic labels into the protein−ligand complex as demonstrated here.

CONCLUSIONS

Time-resolved infrared (TRIR) spectroscopy is a valuable tool with which to study the AppA light-sensing mechanism. This structure-sensitive difference technique enables the observation of very small structural changes in the active site of a complex heterogeneous system. However, isotope labeling is required in order to fully extract all the information contained in the TRIR spectra. Here we report the synthesis and analysis of the [4-$^{18}O_1$]-FAD, [U-$^{15}N_4$]-FAD, [xylene-$^{13}C_8$]-FAD, and [U-$^{13}C_{17}$]-FAD isotopologues and compare the TRIR spectra of these isotope-labeled FADs in solution and bound to d- and $lAppA_{BLUF}$. To our knowledge, the [U-$^{15}N_4$]-FAD, [xylene-$^{13}C_8$]-FAD, and [U-$^{13}C_{17}$]-FAD isotopologues have not been synthesized previously, although [5-$^{15}N_1$]-FAD and [1,3-$^{15}N_2$]-FAD have been previously used for mode assignment.[23,28] Here we use a combination of TRIR data and DFT calculation to unambiguously assign ground-state modes of the isoalloxazine ring in the window of 1500−1750 cm^{-1}, together with an excited-state mode. In general, our data are in good agreement with the existing literature on flavin mode assignment. In particular, the FAD isotopologue [xylene-$^{13}C_8$]-FAD has enabled us to assign modes associated with

the isoalloxazine xylene ring, while [U-$^{13}C_{17}$]-FAD will be useful for differentiating between flavin and protein modes. The sensitivity of the carbonyl localized modes of flavin to hydrogen bonding has been illustrated and contributions to these modes (e.g., N_3H wag and $C_{10a}N_1$ stretch) characterized. Moving forward, the [U-$^{13}C_{17}$]-FAD and [U-$^{15}N_4$]-FAD isotopologues will be useful for assigning bands associated with flavin radicals that may be formed on the reaction pathway leading from d- to lAppA, or by excitation of the photoinactive light state. The increased understanding of the FAD vibrational spectrum together with the new FAD isotopologues described in the present study will thus play an essential role in future TRIR studies that ultimately lead to a more detailed mechanistic understanding of the AppA photocycle.

■ ASSOCIATED CONTENT

Supporting Information

Mass spectra of FAD isotopologues [U-$^{15}N_4$]-FAD, [4-$^{18}O_1$]-FAD, [xylene-$^{13}C_8$]- FAD and [U-$^{13}C_{17}$]-FAD, and TRIR spectrum of [4-$^{18}O_1$]-FAD in solution. This material is available free of charge via the Internet at http://pubs.acs.org.

■ AUTHOR INFORMATION

Corresponding Author

*Tel.: (631) 632-7907 (P.J.T.); 44(0)1603 593141 (S.R.M.). Fax: (631) 632-7960 (P.J.T.); 44(0)1603 592004 (S.R.M.). E-mail: ptonge@notes.cc.sunysb.edu (P.J.T.); s.meech@uea.ac.uk (S.R.M.).

Notes

The authors declare no competing financial interest.

■ ACKNOWLEDGMENTS

Funded by the EPSRC (EP/G002916 to SRM) and NSF (CHE-0822587 to P.J.T.). We are grateful to STFC for access to the ULTRA laser facility and A.B. thanks the Hans-Fischer-Gesellschaft for support.

■ REFERENCES

(1) Rockwell, N. C.; Su, Y. S.; Lagarias, J. C. *Annu. Rev. Plant Biol.* **2006**, *57*, 837.
(2) Filipek, S.; Stenkamp, R. E.; Teller, D. C.; Palczewski, K. *Annu. Rev. Physiol.* **2003**, *65*, 851.
(3) Kort, R.; Hoff, W. D.; Van West, M.; Kroon, A. R.; Hoffer, S. M.; Vlieg, K. H.; Crielaand, W.; Van Beeumen, J. J.; Hellingwerf, K. J. *Embo J.* **1996**, *15*, 3209.
(4) Losi, A. *Photochem. Photobiol. Sci.* **2004**, *3*, 566.
(5) Briggs, W. R.; Christie, J. M.; Salomon, M. *Antioxid. Redox Signal* **2001**, *3*, 775.
(6) Essen, L. O. *Curr. Opin. Struct. Biol.* **2006**, *16*, 51.
(7) Gomelsky, M.; Klug, G. *Trends Biochem. Sci.* **2002**, *27*, 497.
(8) Anderson, S.; Dragnea, V.; Masuda, S.; Ybe, J.; Moffat, K.; Bauer, C. *Biochemistry* **2005**, *44*, 7998.
(9) Laan, W.; van der Horst, M. A.; van Stokkum, I. H.; Hellingwerf, K. J. *Photochem. Photobiol.* **2003**, *78*, 290.
(10) Stelling, A. L.; Ronayne, K. L.; Nappa, J.; Tonge, P. J.; Meech, S. R. *J. Am. Chem. Soc.* **2007**, *129*, 15556.
(11) Lukacs, A.; Haigney, A.; Brust, R.; Zhao, R. K.; Stelling, A. L.; Clark, I. P.; Towrie, M.; Greetham, G. M.; Meech, S. R.; Tonge, P. J. *J. Am. Chem. Soc.* **2011**, *133*, 16893.
(12) Tishler, M.; Pfister, K.; Babson, R. D.; Ladenburg, K.; Fleming, A. J. *J. Am. Chem. Soc.* **1947**, *69*, 1487.
(13) Haigney, A.; Lukacs, A.; Zhao, R. K.; Stelling, A. L.; Brust, R.; Kim, R. R.; Kondo, M.; Clark, I.; Towrie, M.; Greetham, G. M.; Illarionov, B.; Bacher, A.; Romisch-Margl, W.; Fischer, M.; Meech, S. R.; Tonge, P. J. *Biochemistry* **2011**, *50*, 1321.
(14) Greetham, G. M.; Burgos, P.; Cao, Q.; Clark, I. P.; Codd, P. S.; Farrow, R. C.; George, M. W.; Kogimtzis, M.; Matousek, P.; Parker, A. W.; Pollard, M. R.; Robinson, D. A.; Xin, Z. J.; Towrie, M. *Appl. Spectrosc.* **2010**, *64*, 1311.
(15) Frisch, M. J.; Trucks, G. W.; Schlegel, H. B.; Scuseria, G. E.; Robb, M. A.; Cheeseman, J. R.; Montgomery, J. A., Jr.; Vreven, T.; Kudin, K. N.; Burant, J. C.; Millam, J. M.; Iyengar, S. S.; Tomasi, J.; Barone, V.; Mennucci, B.; Cossi, M.; Scalmani, G.; Rega, N.; Petersson, G. A.; Nakatsuji, H.; Hada, M.; Ehara, M.; Toyota, K.; Fukuda, R.; Hasegawa, J.; Ishida, M.; Nakajima, T.; Honda, Y.; Kitao, O.; Nakai, H.; Klene, M.; Li, X.; Knox, J. E.; Hratchian, H. P.; Cross, J. B.; Adamo, C.; Jaramillo, J.; Gomperts, R.; Stratmann, R. E.; Yazyev, O.; Austin, A. J.; Cammi, R.; Pomelli, C.; Ochterski, J. W.; Ayala, P. Y.; Morokuma, K.; Voth, G. A.; Salvador, P.; Dannenberg, J. J.; Zakrzewski, V. G.; Dapprich, S.; Daniels, A. D.; Strain, M. C.; Farkas, O.; Malick, D. K.; Rabuck, A. D.; Raghavachari, K.; Foresman, J. B.; Ortiz, J. V.; Cui, Q.; Baboul, A. G.; Clifford, S.; J.Cioslowski, Stefanov, B. B.; Liu, G.; Liashenko, A.; Piskorz, P.; Komaromi, I.; Martin, R. L.; Fox, D. J.; Keith, T.; Al-Laham, M. A.; Peng, C. Y.; Nanayakkara, A.; Challacombe, M.; Gill, P. M. W.; Johnson, B.; Chen, W.; Wong, M. W.; Gonzalez, C.; Pople, J. A. *Gaussian 03, Revision A.1*; Gaussian, Inc.: Pittsburgh, PA, 2003.
(16) Scott, A. P.; Radom, L. *J. Phys. Chem.* **1996**, *100*, 16502.
(17) Kondo, M.; Nappa, J.; Ronayne, K. L.; Stelling, A. L.; Tonge, P. J.; Meech, S. R. *J. Phys. Chem. B* **2006**, *110*, 20107.
(18) Abe, M.; Kyogoku, Y.; Kitagawa, T.; Kawano, K.; Ohishi, N.; Takaisuzuki, A.; Yagi, K. *Spectrochim. Acta A* **1986**, *42*, 1059.
(19) Abe, M.; Kyogoku, Y. *Spectrochim. Acta A* **1987**, *43*, 1027.
(20) Kitagawa, T.; Nishina, Y.; Kyogoku, Y.; Yamano, T.; Ohishi, N.; Takai-Suzuki, A.; Yagi, K. *Biochemistry* **1979**, *18*, 1804.
(21) Wu, J.; Bell, A. F.; Luo, L.; Stephens, A. W.; Stankovich, M. T.; Tonge, P. J. *Biochemistry* **2003**, *42*, 11846.
(22) Kim, M.; Carey, P. R. *J. Am. Chem. Soc.* **1993**, *115*, 7015.
(23) Nishina, Y.; Sato, K.; Miura, R.; Matsui, K.; Shiga, K. *J. Biochem.* **1998**, *124*, 200.
(24) Bowman, W. D.; Spiro, T. G. *Biochemistry* **1981**, *20*, 3313.
(25) Eisenberg, A. S.; Schelvis, J. P. *J. Phys. Chem. A* **2008**, *112*, 6179.
(26) Copeland, R. A.; Spiro, T. G. *J. Phys. Chem.* **1986**, *90*, 6648.
(27) Unno, M.; Kikuchi, S.; Masuda, S. *Biophys. J.* **2010**, *98*, 1949.
(28) Hazekawa, I.; Nishina, Y.; Sato, K.; Shichiri, M.; Miura, R.; Shiga, K. *J. Biochem.* **1997**, *121*, 1147.
(29) Wolf, M. M.; Zimmermann, H.; Diller, R.; Domratcheva, T. *J. Phys. Chem. B* **2011**, *115*, 7621.
(30) Unno, M.; Kumauchi, M.; Sasaki, J.; Tokunaga, F.; Yamauchi, S. *Biochemistry* **2002**, *41*, 5668.
(31) Unno, M.; Sano, R.; Masuda, S.; Ono, T. A.; Yamauchi, S. *J. Phys. Chem. B* **2005**, *109*, 12620.
(32) Tonge, P. J.; Pusztai, M.; White, A. J.; Wharton, C. W.; Carey, P. R. *Biochemistry* **1991**, *30*, 4790.